The effects of electron temperature in terahertz quantum cascade laser predictions

Philip Slingerland[a], Christopher Baird[a], Bryan Crompton[a], Robert Giles[a] and William E. Nixon[b]

[a]Submillimeter-Wave Technology Laboratory,
University of Massachusetts Lowell, 175 Cabot St Lowell, MA 01854;
[b]U. S. Army National Ground Intelligence Center,
2055 Boulders Rd Charlottesville, VA 22911

ABSTRACT

Quantum cascade lasers (QCL's) employ the mid- and far-infrared intersubband radiative transitions available in semiconducting heterostructures. Through the precise design and construction of these heterostructues the laser characteristics and output frequencies can be controlled. When fabricated, QCL's offer a lightweight and portable alternative to traditional laser systems which emit in this frequency range. The successful operation of these devices strongly depends on the effects of electron transport. Studies have been conducted on the mechanisms involved in electron transport and a prediction code for QCL simulation and design has been completed. The implemented approach utilized a three period simulation of the laser active region. All of the wavefunctions within the simulation were included in a self-consistent rate equation model. This model employed all relevant types of scattering mechanisms within three periods. Additionally, an energy balance equation was studied to determine the temperature of electron distributions separately from the lattice temperature. This equation included the influence of both electron-LO phonon and electron-electron scattering. The effect of different modelling parameters within QCL electron temperature predictions will be presented along with a description of the complete QCL prediction code.

Keywords: quantum cascade lasers, terahertz, electron temperature, device modelling

1. INTRODUCTION

A quantum cascade laser (QCL) is a type of semiconductor laser whose emission frequency can be chosen by proper design of the epitaxial layers. QCL's are made by growing alternating layers of varying thickness onto a substrate. Each layer is only a few nanometers thick but still maintains a band-gap between the conduction and valence bands. At the junction of the layers the difference of the conduction band energies forms a potential barrier. These heterostructures establish a series of finite quantum wells that trap electrons. Additionally, a bias voltage is applied which provides electron pumping. In each period of the active region, electrons tunnel through the energy barriers, de-excite, emit a photon, and continue tunneling through to the next period to repeat the process.

Through the design of the heights and thicknesses of these wells, the spacing of allowed electron energy levels and wavefunction shapes can be controlled. By tailoring these energy levels and wavefunctions, a population inversion can be established and lasing can occur. This has been done successfully for wavelengths in the terahertz range, but not at high temperatures[1] (above 150K in cw mode) or with output powers high enough for most practical applications[2] (150 mW in cw mode). Difficulties arise from the small energy spacing between levels required in this frequency range, and from the associated electron dynamics.

The physical mechanisms that affect the performance of a terahertz QCL must be fully understood if current designs are to be improved. Temperature dependence plays a significant part in how electrons are transported through the active region. Due to the small energy spacing between electron energy levels, thermal effects may be particularly harmful to the carefully designed electron populations. Therefore, a detailed understanding of electron scattering mechanisms, electron level populations and the temperature of the electrons should aid in the improvement of active region designs.

Report Documentation Page

Form Approved
OMB No. 0704-0188

1. REPORT DATE	2. REPORT TYPE	3. DATES COVERED
APR 2010		**00-00-2010 to 00-00-2010**

4. TITLE AND SUBTITLE
The effects of electron temperature in terahertz quantum cascade laser predictions

5a. CONTRACT NUMBER
5b. GRANT NUMBER
5c. PROGRAM ELEMENT NUMBER

6. AUTHOR(S)

5d. PROJECT NUMBER
5e. TASK NUMBER
5f. WORK UNIT NUMBER

7. PERFORMING ORGANIZATION NAME(S) AND ADDRESS(ES)
U. S. Army National Ground Intelligence Center,2055 Boulders Rd,Charlottesville,VA,22911

8. PERFORMING ORGANIZATION REPORT NUMBER

9. SPONSORING/MONITORING AGENCY NAME(S) AND ADDRESS(ES)

10. SPONSOR/MONITOR'S ACRONYM(S)
11. SPONSOR/MONITOR'S REPORT NUMBER(S)

12. DISTRIBUTION/AVAILABILITY STATEMENT
Approved for public release; distribution unlimited

13. SUPPLEMENTARY NOTES
in Modeling and Simulation for Defense Systems and Applications V, edited by Eric J. Kelmelis, Proceedings of SPIE Vol. 7705 (SPIE, Bellingham, WA, 2010) 77050C. April 2010

14. ABSTRACT
Quantum cascade lasers (QCL?s) employ the mid- and far-infrared intersubband radiative transitions available in semiconducting heterostructures. Through the precise design and construction of these heterostructues the laser characteristics and output frequencies can be controlled. When fabricated, QCL?s offer a lightweight and portable alternative to traditional laser systems which emit in this frequency range. The successful operation of these devices strongly depends on the effects of electron transport. Studies have been conducted on the mechanisms involved in electron transport and a prediction code for QCL simulation and design has been completed. The implemented approach utilized a three period simulation of the laser active region. All of the wavefunctions within the simulation were included in a self-consistent rate equation model. This model employed all relevant types of scattering mechanisms within three periods. Additionally, an energy balance equation was studied to determine the temperature of electron distributions separately from the lattice temperature. This equation included the influence of both electron-LO phonon and electron-electron scattering. The effect of different modelling parameters within QCL electron temperature predictions will be presented along with a description of the complete QCL prediction code.

15. SUBJECT TERMS

16. SECURITY CLASSIFICATION OF:			17. LIMITATION OF ABSTRACT	18. NUMBER OF PAGES	19a. NAME OF RESPONSIBLE PERSON
a. REPORT	b. ABSTRACT	c. THIS PAGE			
unclassified	**unclassified**	**unclassified**	**Same as Report (SAR)**	**8**	

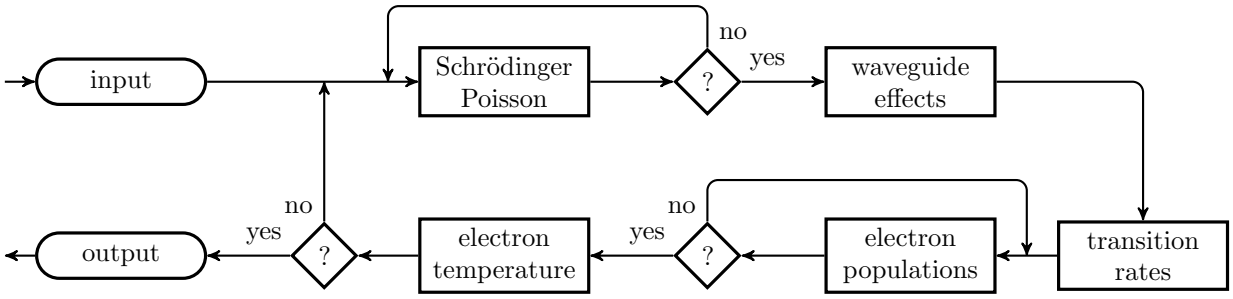

Figure 1: Flow chart of the complete QCL prediction code with electron temperature calculation included. Conditional steps are indicated by a question mark. After the Schrödinger-Poisson box, electron states are checked for convergence. After the electron populations box, electron populations are checked for convergence. After the electron temperature box, the electron temperature is checked for convergence.

2. CODE DESCRIPTION

The QCL prediction code uses a self-consistent semi-classical approach, which involves solving the one-electron Schrödinger equation for electrons in the appropriate effective potential in order to obtain their possible quantum states. The effect of electron-electron interactions is then added in classically by solving the Poisson equation. Solving the Poisson equation yields the built-in potential of the structure, which is then added back into the effective potential used in the Schrödinger equation. The cycle is repeated until a self-consistent solution is obtained. In order to solve the Poisson equation, the charge density, and thus the Fermi levels, must be obtained self-consistently. Once the electron states are found the transition rates can be calculated.

The transition rates for scattering processes are computed in a standard fashion, using Fermi's Golden Rule. This code currently includes electron-photon, electron-phonon and electron-electron scattering. After the transition rates have been found for every possible transition, the code then uses them to determine the electron population densities of each level by solving a set of iterative rate equations. These rate equations are computed following a well-documented procedure.[3] However, in this case, the equations include every possible transition that can occur within three consecutive periods, rather than just focusing on the two lasing states and the near-by injection states in the central period. Additionally, the photon populations are calculated for all possible radiative electron transitions. Finally, the lasing frequency and gain are calculated.

The approach described thus far does not yet take into account the possibility that electrons could have a temperature different than the lattice temperature. And, as mentioned above, this could affect their dynamics within the device, especially in terahertz designs. Therefore, a thorough investigation of electron temperature has been pursued.

Once testing on the electron temperature code is complete, it will add an additional level of consistency to the prediction code. After the electron temperature, T_e, is calculated it will be compared to the lattice temperature, T_l. If different, they are sent back to the beginning of the prediction code as new input parameters, where T_l would be used in any calculations involving the lattice, while T_e will be used in any calculations involving the electrons. The complete code structure is outlined in a flow chart in Fig. 1.

3. ELECTRON TEMPERATURE

3.1 Theory

The method used in this study for determining the average electron temperature of a device follows the one developed by Harrison.[4] It is based on the principle of an energy balance condition: under equilibrium operating conditions, the rate at which electron distributions gain kinetic energy through scattering will balance with the rate at which kinetic energy is lost to the lattice. For the case of phonon emission, the change in kinetic energy of an electron can be written as: $\Delta E = E_i - E_f - E_{\mathrm{LO}}$, where $\Delta E > 0$ represents an increase in kinetic energy while $\Delta E < 0$ represents a decrease in kinetic energy. For phonon absorption, $\Delta E = E_i - E_f + E_{\mathrm{LO}}$. From the calculation of phonon transition rates, the scattering times τ_{if}^{em} and τ_{if}^{abs} are known. The electron population

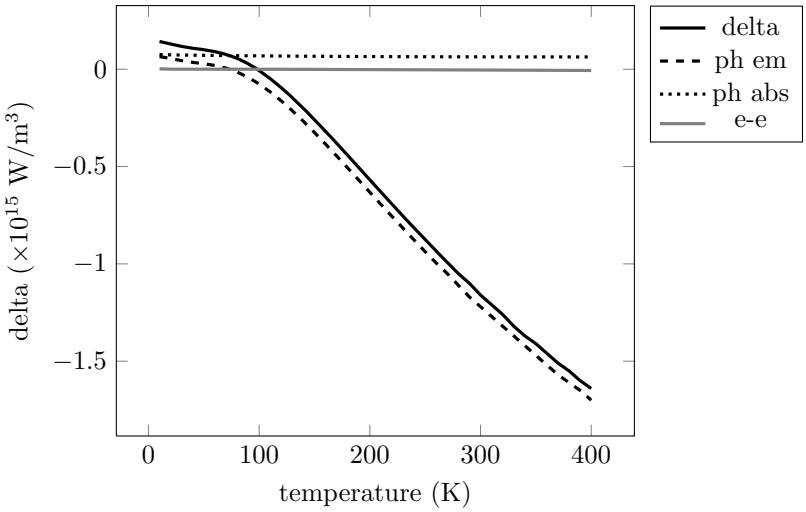

Figure 2: Plot of Δ as a function of temperature for a typical configuration, showing the correct electron temperature as the one at the zero crossing. In this case, $T_e = 83$ K. Also shown are the contributions from phonon emission (ph em), phonon absorption (ph abs) and electron-electron scattering (e-e) to the energy balance equation. These data are calculated for the Sirtori mid-IR structure[5] at a bias voltage of 48 kV/cm and at a lattice temperature of 77 K.

densities n_i, are also known from the solution of the rate equations. Therefore, the net kinetic energy generation rate due to electron-phonon scattering is

$$\sum_f \sum_i \left[\frac{n_i}{\tau_{if}^{\mathrm{em}}}(E_i - E_f - E_{\mathrm{LO}}) + \frac{n_i}{\tau_{if}^{\mathrm{abs}}}(E_i - E_f + E_{\mathrm{LO}}) \right] . \tag{1}$$

This sum includes both interstate ($i \neq f$) and intrastate ($i = f$) scattering. In the case of intrastate scattering, $\Delta E = \pm E_{\mathrm{LO}}$.

For electron-electron scattering, the change in kinetic energy is simply: $\Delta E = E_f - E_i$. The electron-electron scattering transition times $\tau_{if}^{\mathrm{e-e}}$, are also known. Therefore the net kinetic energy generation rate for e-e scattering is

$$\sum_f \sum_i \left[\frac{n_i}{\tau_{if}^{\mathrm{e-e}}}(E_i - E_f) \right] . \tag{2}$$

Eqs. (1) and (2) can be combined into a single equation by generalizing the terms as:

$$\Delta = \sum_{\mathrm{em,abs,e-e}} \sum_f \sum_i \frac{n_i}{\tau_{if}}(E_i - E_f - \delta E) = 0 \, , \tag{3}$$

where δE is equal to $-E_{\mathrm{LO}}$ for phonon emission (em), $+E_{\mathrm{LO}}$ for phonon absorption (abs), and zero for electron-electron (e-e) scattering. It should be noted that electron-photon scattering does not have to be considered in Eq. (3) since the absorption or emission of a photon by an electron negligibly changes its kinetic energy due to conservation of momentum.

The scattering times, τ_{if}, are functions of n_i and the electron temperature. Therefore, n_i and τ_{if} must be calculated over a range of electron temperatures and then used in Eq. (3). Whichever temperature solves the energy balance equation, by leading to the equilibrium state where $\Delta = 0$, is identified as the average electron temperature T_e of the device (see Fig. 2).

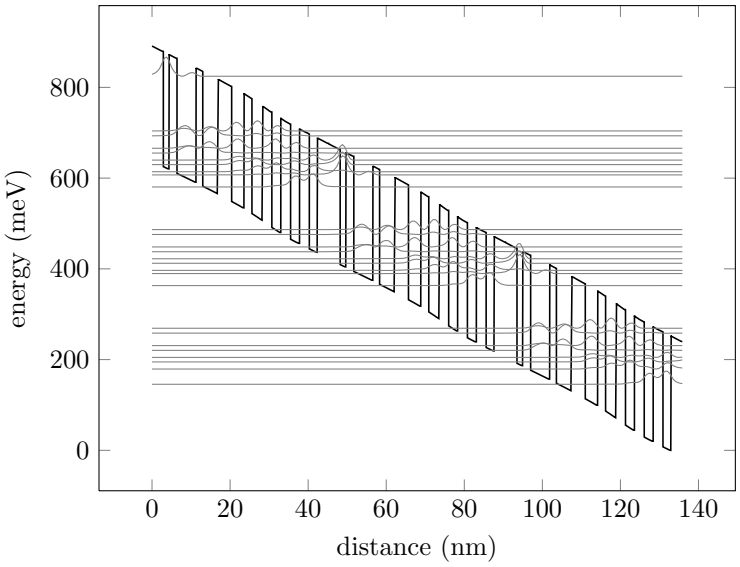

Figure 3: Wavefunctions found in 3 periods of the active region design of Sirtori[5] using an applied bias voltage of 48 kV/cm and at a lattice temperature of 77 K.

3.2 Results and analysis

When originally published by the Harrison group, the method of electron temperature determination was based on the use of 15 states in $1\frac{1}{2}$ periods of the QCL active region.[4] However, if more of the active region is included in QCL simulations it is unclear how much of the active region should be used in T_e calculations. Additionally, if only $1\frac{1}{2}$ periods are used, it is unclear which electron states should be used to make up those $1\frac{1}{2}$ periods. In order to resolve these issues, a study was conducted to observe the effects of using different combinations of states to calculate the electron temperature. As explained below, it was found that these calculations were sensitive to such combinations.

First, an attempt was made to recreate the theoretical results obtained by Harrison.[4] His work studied the mid-IR structure designed and built by Sirtori's group.[5] When the QCL prediction code described in this paper was applied to Sirtori's structure, all three periods were used. The code found 27 states in three periods, as illustrated in Fig. 3. To reconcile the uncertainty of which electron states from $1\frac{1}{2}$ periods to use, all possible combinations of 15 consecutive states were used to calculate T_e. As shown in Table 1, there was a considerable amount of variation. It should also be noted that all of the T_e's are lower than those calculated by Harrison. From these results, it can be concluded that any choice of states in the computation will not lead to the same result. The question arises: What set of states should be chosen to ensure the most accurate electron temperature calculation? See Sec. 3.2.1 for a further examination of this question.

In order to make comparisons with experimental measurements, the Page mid-IR structure[6] was studied as well. The lattice and electron temperatures of this mid-IR QCL have been measured and reported in Ref. 7 where measurements were made over a range of electronic power. However, the voltages used were well below the alignment voltage. Two different heat sink temperatures, 140 K and 243 K, were also used. Comparisons were made between the T_e's calculated using the 3 period prediction code and the reported measurements. Specifically, the design was simulated using the highest values of electric power quoted in the paper at both heat sink temperatures. At $T_H = 140$ K, the highest power used was 7 W. At this point, the measured T_l was 190 K and the measured T_e was 295 K. When simulated with the 3 period QCL prediction code, the calculated T_e was found to be 192 K. At $T_H = 243K$, the highest power used was 3 W. At this point the measured T_l was 265 K and the measured T_e was 330 K. When simulated, the T_e was found to be 270 K. However, it should be noted that in Ref. 7, an offset value was applied to the measured T_e's to take into account heating by a probe laser. Taking this offset value into account would improve the agreement between the measured T_e's and those

Table 1: Electron temperatures calculated for Sirtori's mid-IR QCL design[5] using different sets of electron states. All input parameters into the QCL prediction code were the same as those used by Harrison in his simulation of the same structure.[4] The left column contains the 15 electron states, ψ's, while the remaining columns contain the calculated T_e from using the corresponding collection of ψ's. The lattice temperature T_l and calculated T_e from Harrison's simulations are included above each column.

ψ's	T_l = 77 K T_e = 128 K	T_l = 200 K T_e = 244 K	T_l = 300 K T_e = 363 K
1-15	79	204	315
2-16	85	211	321
3-17	85	213	326
4-18	82	214	329
5-19	84	206	321
6-20	82	214	335
7-21	81	210	327
8-22	79	208	323
9-23	79	206	318
10-24	84	204	315
11-25	85	211	321
12-26	85	213	326
13-27	89	214	329

simulated using the prediction code.

The Page structure was also simulated using bias voltages above threshold. A range of lattice temperatures were used for each bias voltage and the electron temperatures were calculated under these conditions (see Fig. 4). Note that T_e increases linearly with increasing T_l. Also, the calculated T_e's reached higher values compared to the T_e's calculated using below-threshold conditions. Therefore, higher bias voltages lead to higher T_e's, but the relationship is not as linear as that between T_e and T_l.

3.2.1 Deviation in T_e calculations

The T_e data from the study of the Sirtori mid-IR QCL[5] were analyzed further by looking at their standard deviation. First, additional T_e calculations were performed by including more electron states than just 15. Collections of 16, 17, 18, ..., 25, 26, 27 states and all of their possible combinations of consecutive states were used to find T_e as was done using just 15 states. The standard deviation from their average was then determined from each collection of calculated T_e's. It was assumed that the set of states with the lowest standard deviation in T_e would ultimately be the set that best matches the physical world. The results from this study are shown in Fig. 5. It was anticipated that the deviation would consistently decrease as more states are included. Surprisingly, there is a clear minimum in standard deviation when 20 states are used to calculate T_e. This equates to approximately $\frac{3}{4}$ of the total number of states in three periods.

On one hand, including more electron states should more accurately model the physical QCL, which has a large number of states throughout the device, and thus reduce the deviation. On the other hand, including the inaccurate states on the edge of the three period model should degrade the deviation. The minimum in Fig. 5 is the balancing point of these two effects.

Other QCL structures were modeled in order to examine the effect of different electron state combinations on the calculated T_e and the amount of deviation observed. Structures designed by Barbieri[8] and Page[6] were used. Above threshold, the Page structure exhibited very similar behavior to that of Sirtori's structure. A minimum

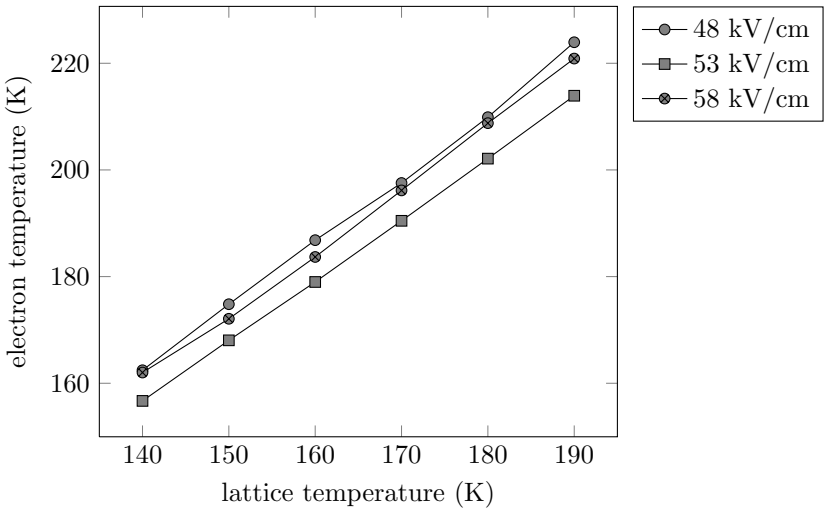

Figure 4: Plot of T_e vs. T_l over a range of bias voltages applied to the Page mid-IR QCL.[6] These voltages are all above threshold.

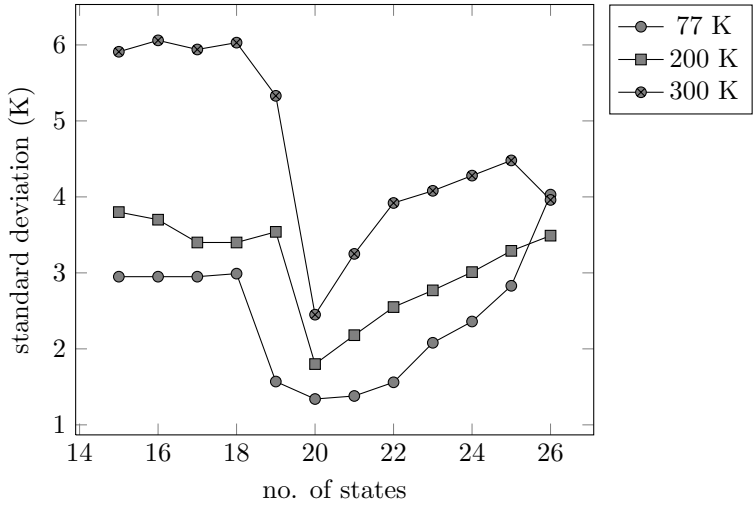

Figure 5: Plot of standard deviation of the calculated electron temperatures as a function of the number of electron states included. Results are shown for three lattice temperatures applied to the Sirtori mid-IR structure[5] at a bias voltage of 48 kV/cm. The standard deviation reaches a minimum when 20 out of the 27 total states are included.

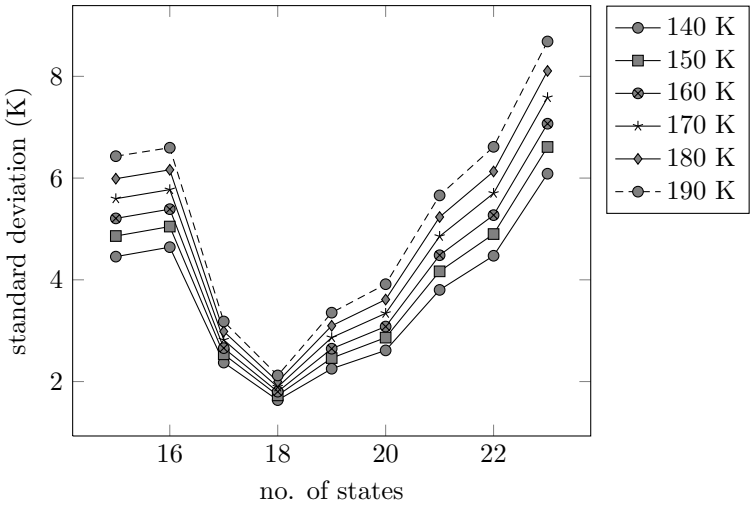

Figure 6: Plot of standard deviation of the calculated electron temperatures as a function of the number of electron states included. Results are shown for six lattice temperatures applied to the Page mid-IR structure[6] at a bias voltage of 53 kV/cm. There is a minimum standard deviation when 18 out of the 24 total states are included.

in standard deviation was observed when 18 of the 24 electron states in three periods were used to calculate T_e (see Fig. 6). This corresponds to exactly $\frac{3}{4}$ of the total number of states.

The Barbieri structure exhibited similar behavior with regards to which fraction of electron states provides the lowest amount of deviation among the possible combinations of consecutive states. However, in some cases the deviation was lowest at a fraction higher than $\frac{3}{4}$ of the total number of electron states. It should also be noted that the mean T_e's that were calculated for the Barbieri structure were lower than the T_l used in the simulations, and so may have had some unaddressed inaccuracies.

4. CONCLUSIONS

When more than $1\frac{1}{2}$ periods of a QCL active region are used in the prediction code, different combinations of 15 electron states produce different calculated values for the average electron temperature (T_e). T_e were found using the energy balance equation (Eq. 3) for each possible combination of 15 states and a standard deviation for the T_e's was found. When more electron states are used to find T_e, the standard deviation changes. For some QCL designs, a particular number of states consistently resulted in a minimum standard deviation. For the case of resonant phonon, mid-IR designs in the above-threshold condition the optimal number of electron states to include in calculations of the electron temperature is $\frac{3}{4}$ of the total number of states.

REFERENCES

[1] Williams, B. S., Kumar, S., and Hu, Q., "Operation of terahertz quantum-cascade lasers at 164 K in pulsed mode and at 117 K in continuous-wave mode," *Opt. Express* **13**, 3331–3339 (2005).

[2] Williams, B. S., Kumar, S., Hu, Q., and Reno, J. L., "High-power terahertz quantum-cascade lasers," *Electron. Lett.* **42**, 89–91 (2006).

[3] Donovan, K., Harrison, P., and Kelsall, R. W., "Self-consistent solutions to the intersubband rate equations in quantum cascade lasers: Analysis of a GaAs/Al_xGa_{1-x}As device," *J. Appl. Phys.* **89**, 3084–3090 (2001).

[4] Harrison, P., Indjin, D., and Kelsall, R. W., "Electron temperature and mechanisms of hot carrier generation in quantum cascade lasers," *J. Appl. Phys.* **92**, 6921–6923 (2002).

[5] Sirtori, C., Kruck, P., Barbieri, S., Collot, P., Nagle, J., Beck, M., Faist, J., and Oesterle, U., "GaAs/Al_xGa_{1-x}As quantum cascade lasers," *Appl. Phys. Lett.* **73**, 3486–3488 (1998).

[6] Page, H., Becker, C., Robertson, A., Glastre, G., Ortiz, V., and Sirtori, C., "300 K operation of a GaAs-based quantum-cascade laser at $\lambda \approx 9$ μm," *Appl. Phys. Lett.* **78**, 3529–3531 (2001).

[7] Spagnolo, V., Scamarcio, G., Page, H., and Sirtori, C., "Simultaneous measurement of the electronic and lattice temperatures in GaAs/$Al_{0.45}Ga_{0.55}As$ in quantum-cascade lasers: influence on the optical performance," *Appl. Phys. Lett.* **84**, 3690–3692 (2004).

[8] Barbieri, S., Alton, J., Beere, H. E., Fowler, J., Linfield, E. H., and Ritchie, D. A., "2.9 THz quantum cascade lasers operating up to 70 K in continuous wave," *Appl. Phys. Lett.* **85**, 1674–1676 (2004).